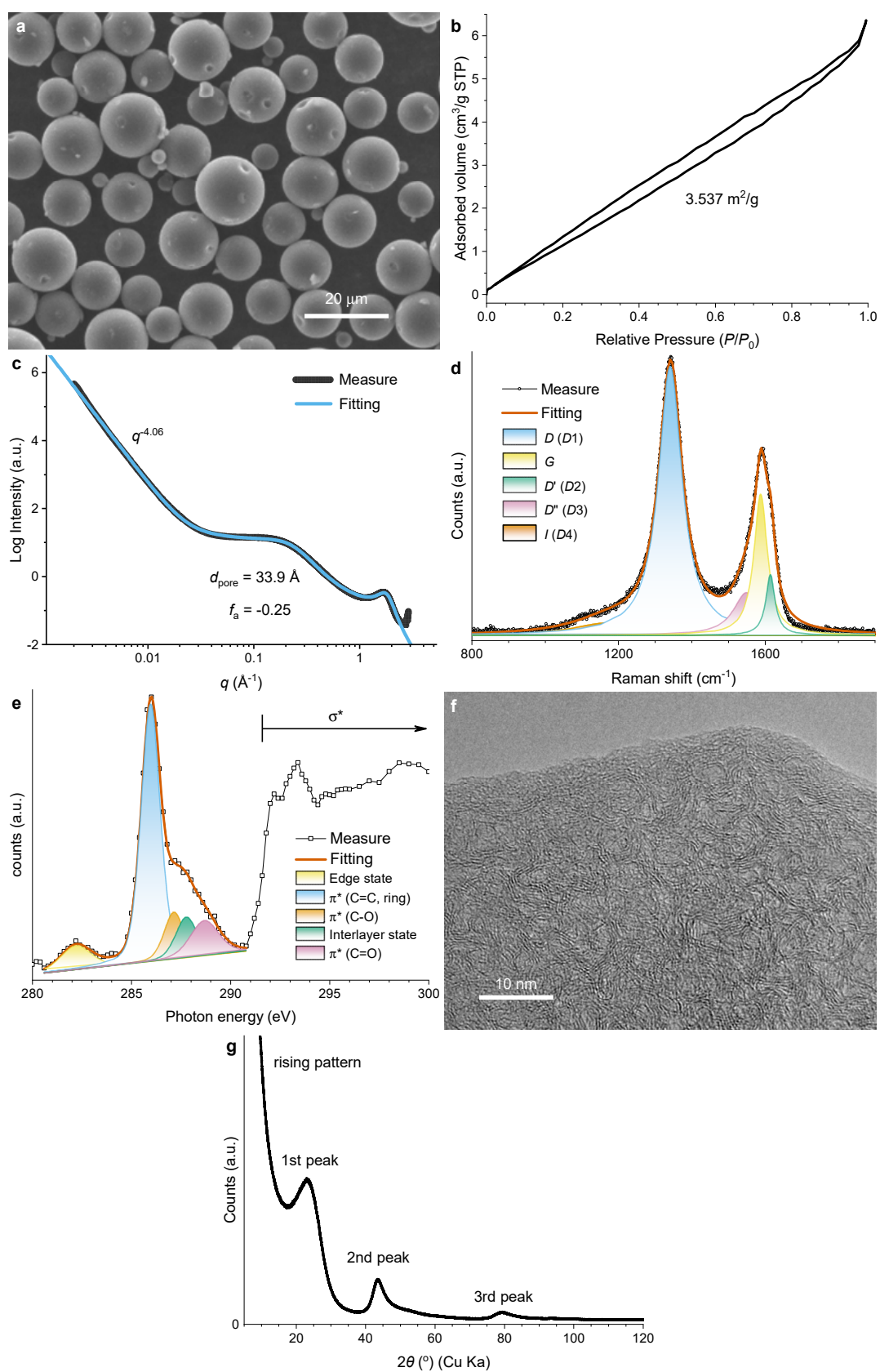
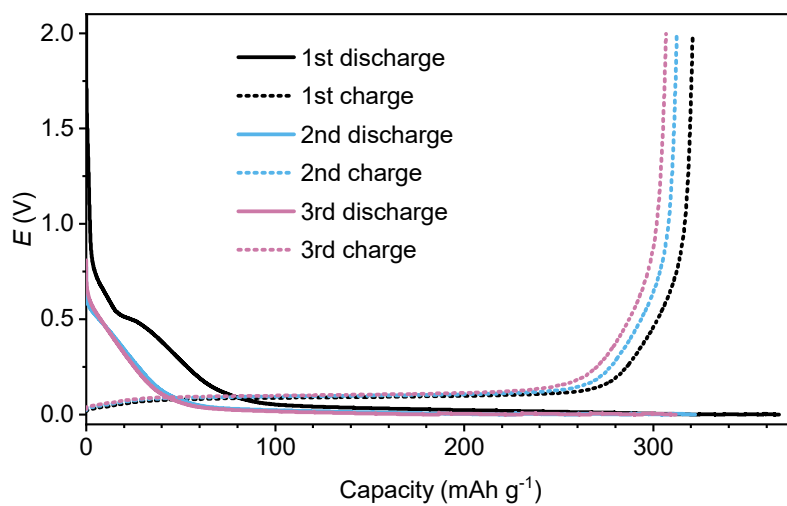


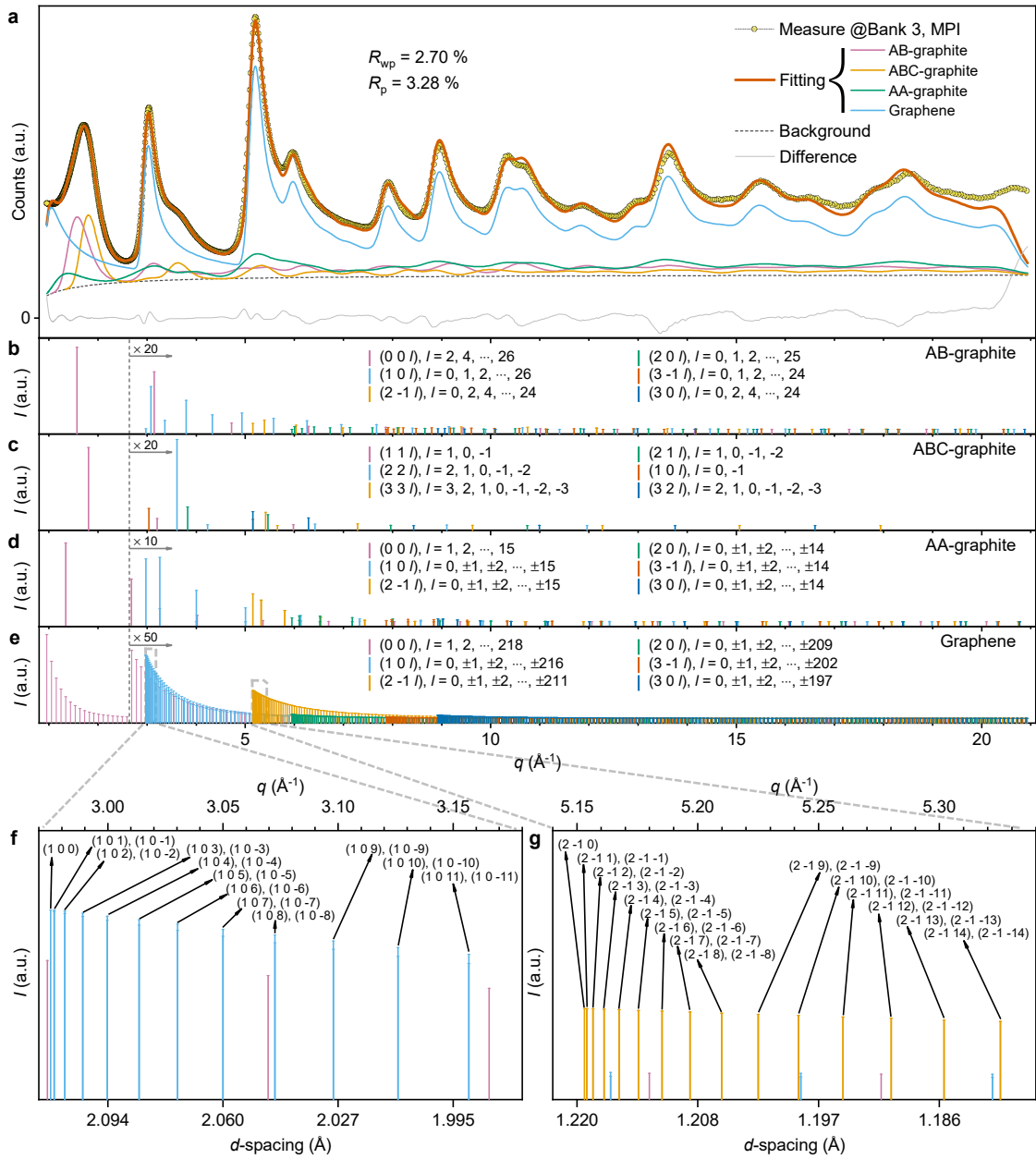
Extended Data Figures



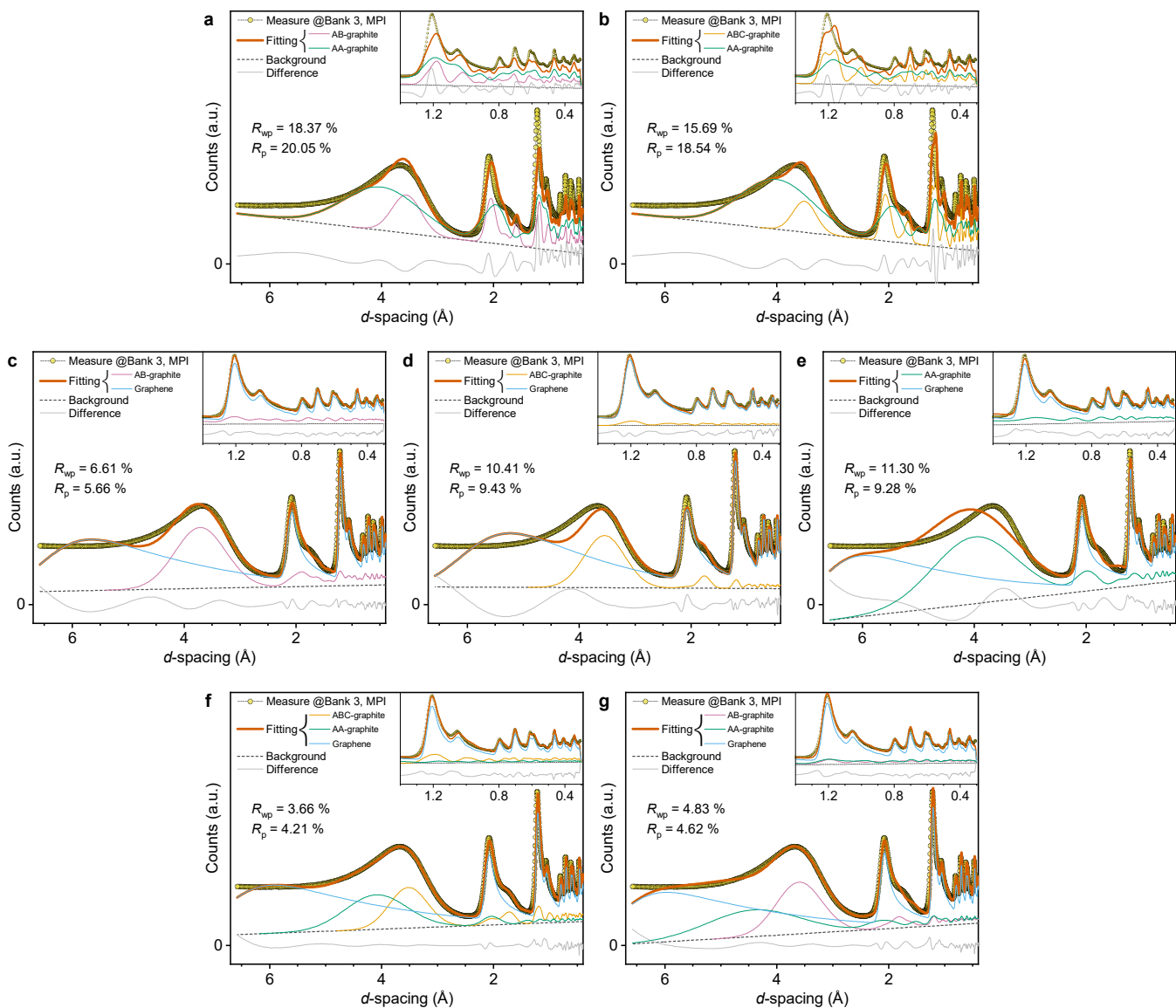
Extended Data Fig. 1 | General characterization of KC15. a, SEM, b, BET, c, SAXS and its fitting results, d, Raman spectra and its fitting results, e, XAS and its fitting results, f, TEM, and g, XRD.



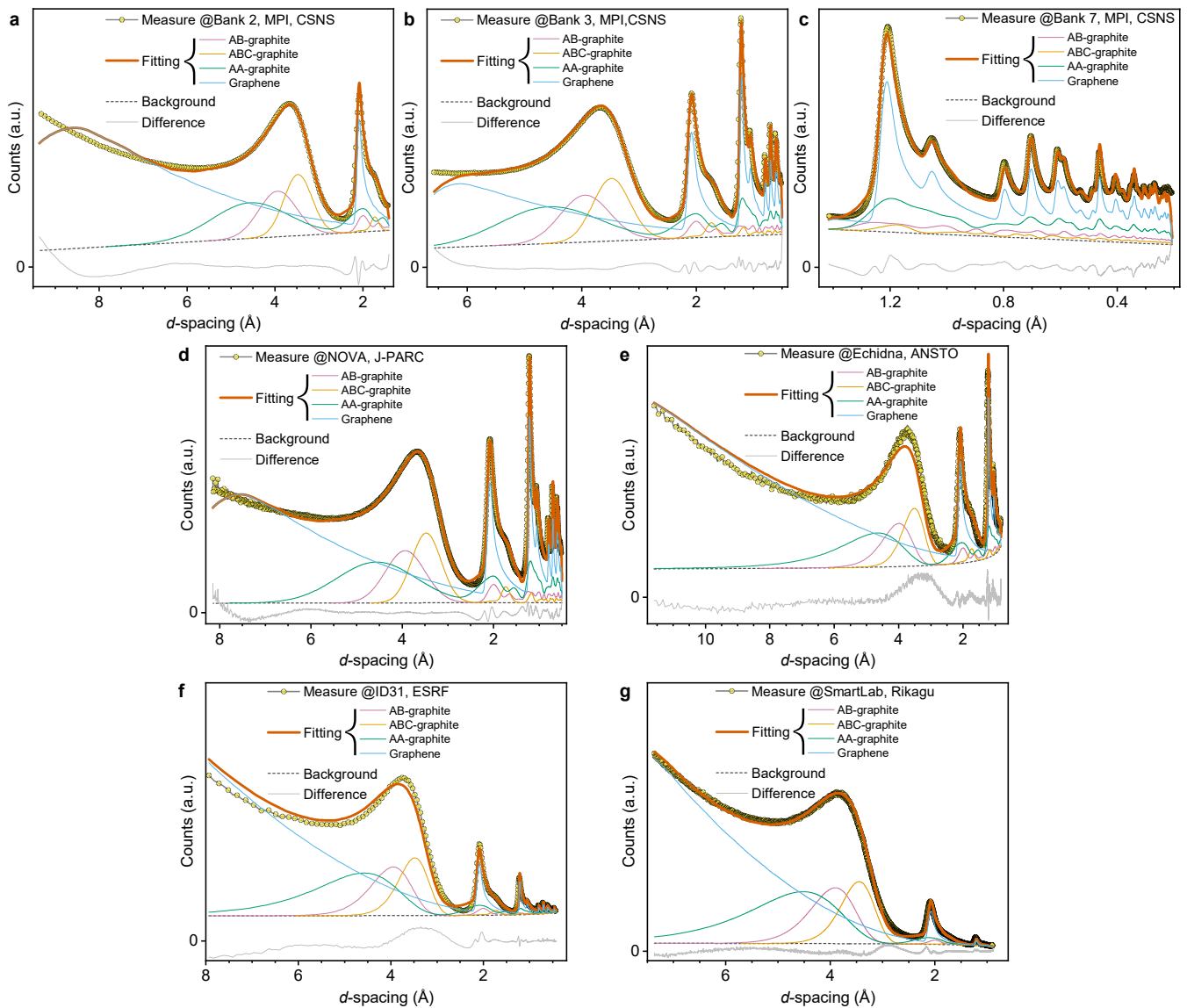
Extended Data Fig. 2 | Electrochemical test results of KC15.



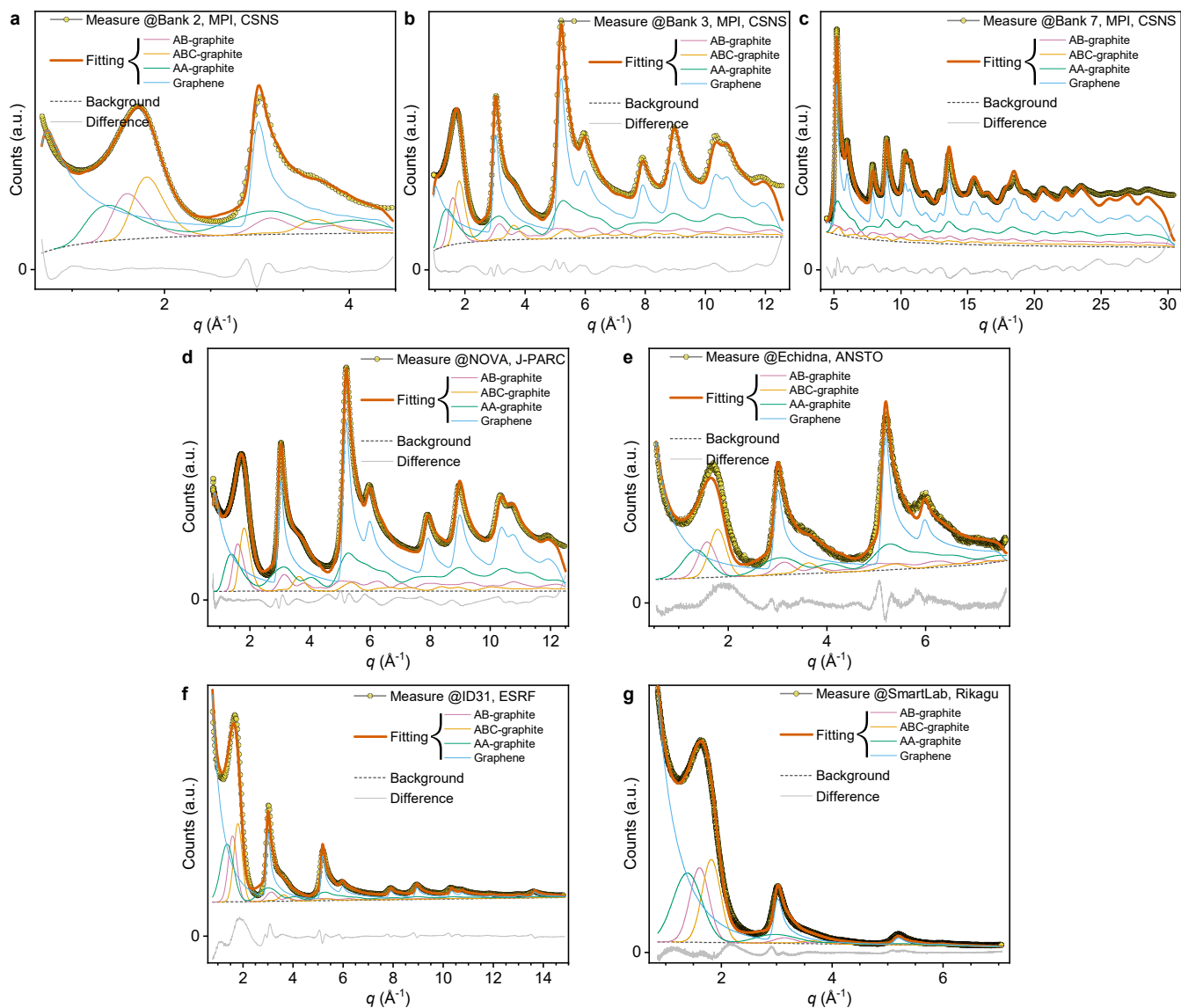
Extended Data Fig. 3 | Final Rietveld refinement solution for ND data of KC15 shown in q , as referenced to Fig. 1d-h. a, Rietveld refinement results and corresponding Miller indices for b, AB-graphite, c, ABC-graphite, d, AA-graphite, and e, graphene. Localized zooms of the Miller index series f, $(1\ 0\ l)$ and g, $(2\ -1\ l)$ for the graphene phase shown in (e).



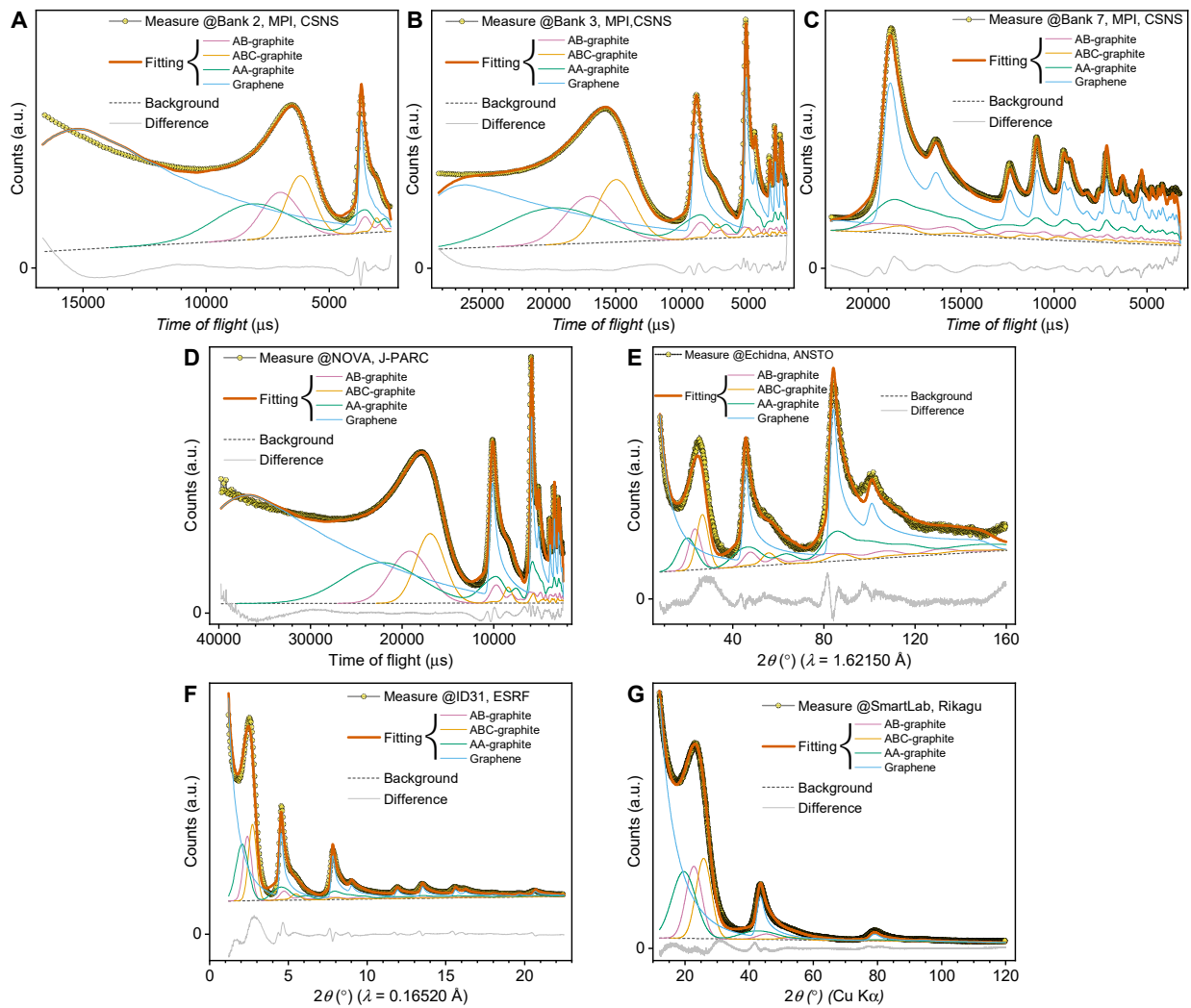
Extended Data Fig. 4 | Remaining phase combinations evaluated during initial Rietveld refinements of a single neutron diffraction dataset (Bank 3, MPI, CSNS) for KC15, supplementing those presented in Fig. 1.



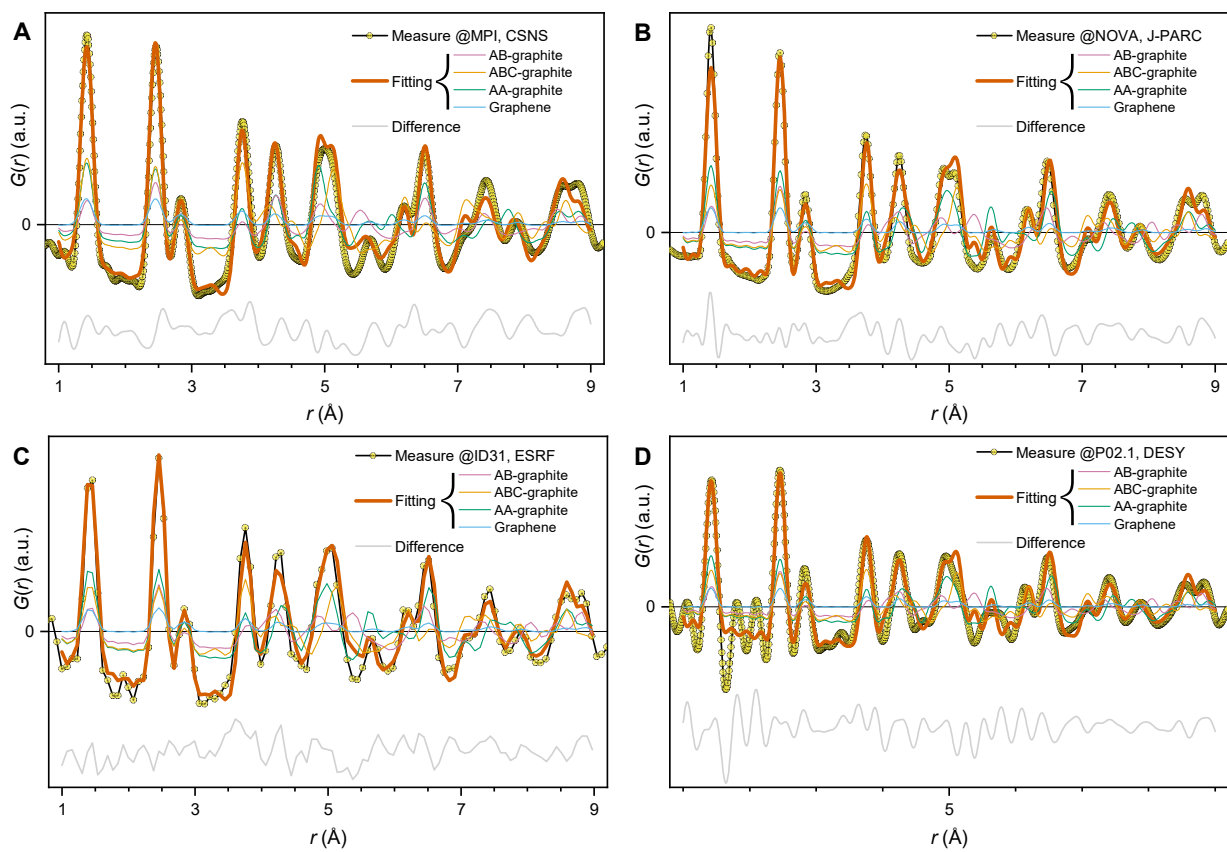
Extended Data Fig. 5 | Results of neutron/X-ray combined Rietveld refinement of KC15 shown in d -spacing. The diffraction patterns and their fitting results of **a**, Bank 2, **b**, Bank 3, and **c**, Bank 7 at MPI, CSNS (TOF-ND); **d**, NOVA at J-PARC (TOF-ND); **e**, Echidna at ANSTO (CW-ND); **f**, ID31 at ESRF (synchrotron-based XRD); and **g**, SmartLab of Rikagu (lab-based XRD).



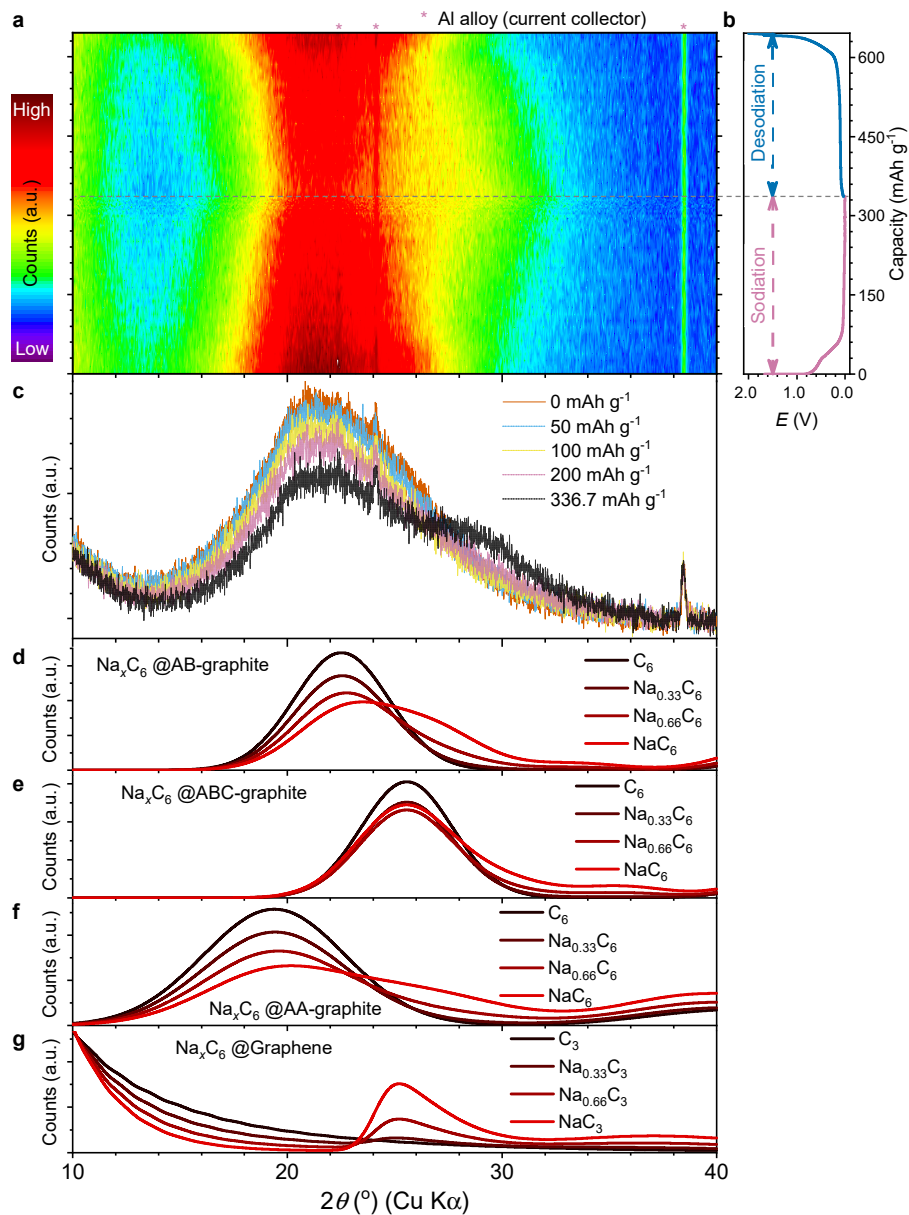
Extended Data Fig. 6 | Results of neutron/X-ray combined Rietveld refinement of KC15 shown in q . The diffraction patterns and their fitting results of **a**, Bank 2, **b**, Bank 3, and **c**, Bank 7 at MPI, CSNS (TOF-ND); **d**, NOVA at J-PARC (TOF-ND); **e**, Echidna at ANSTO (CW-ND); **f**, ID31 at ESRF (synchrotron-based XRD); and **g**, SmartLab of Rikagu (lab-based XRD).



Extended Data Fig. 7 | Results of neutron/X-ray combined Rietveld refinement of KC15 shown in TOF or 2θ . The diffraction patterns and their fitting results of **a**, Bank 2, **b**, Bank 3, and **c**, Bank 7 at MPI, CSNS (TOF-ND); **d**, NOVA at J-PARC (TOF-ND); **e**, Echidna at ANSTO (CW-ND); **f**, ID31 at ESRF (synchrotron-based XRD); and **g**, SmartLab of Rikagu (lab-based XRD).



Extended Data Fig. 8 | Neutron/X-ray combined PDF refinement for KC15. The PDF patterns and their fitting results of **a**, MPI at CSNS (TOF neutron), **b**, NOVA at J-PARC (TOF neutron), **c**, ID31 at ESRF (synchrotron-based X-ray), **d**, P02.1 at DESY (synchrotron-based X-ray).



Extended Data Fig. 9 | Structural evolution of KC15 during sodiation/desodiation characterised by *in situ* XRD. **a**, *In situ* XRD patterns of KC15 during the first sodiation/desodiation cycle, along with **b**, corresponding electrochemical profile and **c**, selected XRD patterns from (**a**) presented as counts versus *d*-spacing plots for clearer reference. Simulated XRD patterns of sodiated phases with varying sodiation concentrations, derived from the host phases of **d**, AB-graphite, **e**, ABC-graphite, **f**, AA-graphite, and **g**, graphene.